FEAT JOURNAL
FARM ENGINEERING AND AUTOMATION TECHNOLOGY JOURNAL
วารสารวิศวกรรมฟาร์มและเทคโนโลยีการควบคุมอัตโนมัติ

Experimental Study on the Performances, Energy Efficiency and Emissions of Porous Burner

*Ditthaphat Tanpradit and Wasan Theansuwan
Division of Mechanical Engineering, Faculty of Engineering, Rajamangala University of Technology Krungthep

Received: 22 October 2019
Revised: 11 December 2019
Accepted: 28 April 2020
Available online: 30 June 2020

Abstract

This research is to experimentally study the performance of a porous burner (PB) and the results are compared with those obtained from the conventional burner (CB). The porous burner consists of two co-concentric cylindrical tubes as a shell and tube heat exchanger. The inside of a tube fills up with spherical ceramics with a diameter of 1.5 cm for forming the porous chamber, which is wrapped around by a larger cylindrical tube as a shell. The shell contains water and serves as a water container. The LPG is used as a fuel and a heat-load condition is set as the gas flow rate of LPG, which is varied in a range of 1 to 7 LPM. Air entrainment is controlled for the excess oxygen between 6-7% in the exhaust. Also, the porosity is a constant of 0.5 and the gas pressure keeps constant at 0.4 bar. Through analysis and discussion of this study, the interesting findings can be drawn as follows: 1) the combustion temperature of the PB is 30% higher than that of the CB on average, while the exhaust gas temperature of the PB is 19% lower than that of the CB on average. 2) Based on the efficiency evaluation, the latent energy, the rate of vaporization, and thermal efficiency obtained by the PB are higher than those obtained by the CB with a value of 46%, 56%, and 48.7% respectively. 3) The maximum energy saving of the PB is higher than that of the CB as much as 21%. 4) very low CO emissions are noticed for both types at high loads, while the NOx emission of the PB is 75% lower than that of the CB and the NOx emission of the PB is lower a 20-ppm limit for all load conditions.

Keywords : Porous Burner Energy Vaporization

* Corresponding author: ditthaphat.t@mail.rmutk.ac.th, Tel.: +66 88 368 0368, fax: +6 662 287 9600

1. Introduction

The porous media combustion is a technique to enhance the combustion efficiency, thereby reducing fuel consumption and being environmentally friendly [1-4]. Several considerable benefits such as stability of flame, high flame speed, and very lean mixture combustion are brought through the feasibility of this combustion. Besides, exhaust gas emission discharged by this combustion is low, especially NO_x [4-6]. Hence, these benefits have been widely used to improve thermal processes. Jinhua et al. [7] studied the experiment on a porous media gas-fired boiler. It was founded that the efficiency of heat transfer could increase to 90%, while the emission of NO_x was less than 45 mg/m^3. The pressure drop was less than 0.001 MPa and also reduced the combustion chamber to be a smaller size. Barcellos et al. [8] studied the ultra-low-emission steam boiler with a reciprocal flow porous burner. Their results revealed that thermal efficiency increased as much as 90%, while the amounts of NO_x and CO were limited to 1.0 and 0.5 ppm, respectively. Sumrerng Jugjai and Viriya Nungniyom [9] studied a porous combustor-heater (PCH) with cyclic flow reversal combustion (CFRC). The optimal switching period under high thermal efficiency and low emission was determined. Their results indicated thermal efficiency as high as 85% with low emissions of CO and NO_x about 200 and 20 ppm, respectively. Recently, Aekkaphon Chaelek, Usa Makmool Grare, and Sumrerng Jugjai [10] proposed a novel design of an atmospheric gas burner using the concept of heat recirculation by porous media combustion technology. With this design, the thermal efficiency could reach a maximum of 51% with less energy consumption about 28.6%, including low emissions. So far, many works of open literature have revealed that the porous medium combustion is a new combustion technique that contributes more advantages to the boiler and burner applications. Therefore, this research was carried out using the concept of porous media combustion techniques through the burner simulation. Results in terms of the capability to produce steam in the porous burner, combustion temperature, heat power output, fuel consumption, and the amount of CO and NO_x in the exhaust gas were presented. Also, these results were compared with the results obtained by the conventional burner.

2. Design and Calculation

2.1 Porosity calculation

The porosity (ε), which is the ratio of space volume in porous material to the total volume (V_d), is shown in Fig. 1. The space volume in the porous material can be determined by subtracting the volume of spherical ceramic (V_{sp}) from the total volume (V_d) ,as seen in Eqs. (1)-(2). Then, the porosity can be calculated from Eq. (3), where n is the number of spherical ceramics. As seen in fig 1, the change in the diameter of ceramic (d_{sp}) causes the difference in the porosity, diameter (D), and height (L) of the chamber and Eq. (4) mathematically expresses this relation. Simplifying Eq. (4) by substituting A_R and L_d into Eq. (4), it can be rearranged as Eq. (5). It should be noted that the value of the porosity is limited in a range of 0 to 1. For the current study, the spherical ball is used to simulate the porous media in the combustion chamber.

$$V_d = \frac{\pi D^2 L}{4} \quad (1)$$

$$V_{sp} = \frac{4}{3}\left(\frac{\pi d_{sp}^{\ 3}}{8}\right) = \frac{\pi d_{sp}^{\ 3}}{6} \quad (2)$$

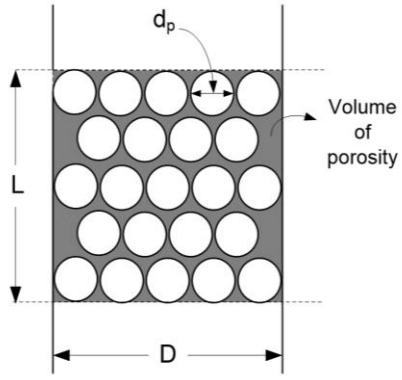

Fig. 1 Porous medium in layer

$$\varepsilon = \frac{V_d - nV_{sp}}{V_d} = 1 - n\frac{V_{sp}}{V_d} \quad (3)$$

$$\varepsilon = 1 - \frac{2n}{3L}\left(\frac{d_{sp}^{\ 3}}{D^2}\right) \quad (4)$$

$$\varepsilon = 1 - \frac{2n}{3L_d (A_R)^2} \quad (5)$$

The inside of the preheat chamber contains the small size of ceramic to protect the propagation of flame in this area. The Peclet number (Pe) expressed in Eq. (6) is defined for this propagation and this dimensionless number should be less than 65 [9].

$$Pe = \frac{d_p S_L \rho_f c_{pf}}{\lambda_f} \quad (6)$$

2.2 Porous burner design

This sub-topic explains how to build the burner. The burner is designed by CAD software. It is divided into four parts i.e. 1) preheat chamber (D), 2) combustion chamber (B), 3) water container (C), and 4) exhaust pipe (A). The porous burner structure is made of stainless steel (SUS 341). The concept design of the porous burner is a shell-tube heat exchanger. The porous burner consists of two co-concentric cylindrical tubes. The inside of a tube fills up with the spherical ceramic to form the porous chamber, which was wrapped around by a larger cylindrical tube as a shell. This shell contains water and serves as a water container. All assemblies of the porous burner are illustrated in Fig.2.

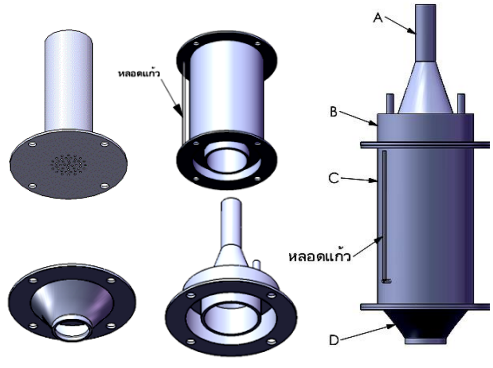

Fig. 2 The assembly of porous burner

2.3 Performance calculation

The performance of the porous burner is presented in terms of the efficiency of vaporization and energy saving (ES). They are calculated from Eqs. (7) – (9) under the assumption that the latent heat condition is only considered.

$$\dot{Q}_{in} = \dot{m}_f (LHV) \quad (7)$$

$$\eta_v = \frac{m_v h_{fg}}{\dot{m}_f (LHV)(\Delta t)} \quad (8)$$

$$ES = \frac{\dot{Q}_{PB} - \dot{Q}_{CB}}{\dot{Q}_{in}} \times 100 \quad (9)$$

3. Research Methodology

3.1 Devices and equipment

All devices and equipment used for research can be divided into six sections, as shown in Fig. 4. At first, the fuel supply system is a 15-kg LPG tank installed with the regulator that is located on the digital weight scale with a resolution of 1 gram. The rotameter is used for adjusting the gas flow rate in a range of 1 – 10 LPM with an accuracy of +/- 2.0%.

Secondly, a 0.5-hp blower that is connected with the control valve is used as the air supply section. Then, the air flows through the pitot tube, and pressure differences are measured to calculate the air-flow rate. Thirdly, the preheat section consists of a mixing chamber and the preheat chamber. The fuel and air are mixed homogeneously within the mixing chamber and then the mixing fluid flows into the preheat chamber that the ceramics are installed. For the present study, ceramics with a small size of 5-mm diameter result in the Peclet number less than 65, as shown in Fig. 3(a), and the secondary air entrance would be this area. Also, this zone is heated up by heat radiation from the combustion process.

Fourthly, the cylindrical chamber made of stainless steel (sus 341) is installed and served as the combustion section. The chamber contains ceramics with a diameter of 15 mm. to maintain the porosity of 0.55 as shown in Fig 3(b).

(a) (b)

Fig. 3 Ceramics of (a) small size (5 mm dia.) and (b) larger size (15 mm of dia.)

The compositions of the ceramic are 92.5% of Al_2O_3, 0.3% of SiO_2, 0.2% of Fe_2O_3, and 5.5% of CaO. This ceramic can resist the high temperature up to 1750°C. The thermal conductivity of the ceramic is in a range of 1.7 – 4.2 W/m·K. At the combustion section, thermocouples are used to probe the temperature at 10 locations along the vertical line of the center of the chamber, specifically, the thermocouples type K for 7 locations and type N for3 locations. These thermocouples have a resolution of 0.001 °C with an accuracy of +/- 0.015°C within the temperature range of -200 °C to +800°C. The thermocouples are connected to 16 channels of Yokogawa's data logger MV2000 for monitoring and recording the result. In addition, the spark plug is located at the bottom of this chamber to initiate the flame in the combustion zone. Fifthly, the feedwater system is provided to supply the 5-L water from the stainless tank to the inlet of a shell at the bottom of the porous burner with a 12-V and 0.5-hp pump. When the water flows into the shell of the porous burner, the water level can be observed through a level sight glass at the wall. Also, there are two holes for a steam vent at the top of the porous burner. Finally, the probe of the Testo 340 combustion analyzer is installed in the exhaust

section to measure the numbers of O_2, CO, and NO_x. It should be noted that O_2 can be measured in a range of 0-25% with an accuracy of +/- 0.12% by volume and tolerance of +/-0.21% by volume. The amount of CO can be measured from 0 – 10,000 ppm with an accuracy of +/- 4 ppm and tolerance of +/-50.75 ppm. The NO_x measurement can be done with an accuracy of +/- 2 ppm and tolerance +/-8.2 ppm. To ensure accurate measurements, all equipment is always calibrated before testing.

3.2 Procedure of experiment

The procedure of the experiment can be explained by Fig. 4. At first, all equipment is installed and checked for its availability. Then, the surrounding conditions and weight of the LPG tank are measured and recorded. Later, the gas valve (No, 3) is opened and the pressure regulator is used to maintain the pressure at 0.4 bars, then the airflow valve (No. 6) is opened and the blower (No. 13) is turned on to operate. After that, the fuel and air will be mixed in the mixing chamber (No. 14). Subsequently, the spark ignition (No. 12) in the combustion zone is started. To ensure that the experiment is conducted under the steady-state condition, the temperature profile is observed with the monitor (No. 21). After reaching the steady-state condition, the testing conditions are set as listed in Table 1. At first condition, the fuel flow rate is set to be 1 LPM using the gas flow meter (No. 5). The fuel consumption rate is measured from the digital weight scale every 5 minutes. Finally, the airflow rate is adjusted by a valve (No. 6) until the excess O_2 reached 7% at the exhaust pipe (No. 19), and then the amounts of CO and NO_x are recorded into the combustion analyzer (No. 20). It should be taken time to be steady-state again for all parameters. It should be noted that before starting a new test, it must be sure that the system can operate under a safe situation and all equipment keeps working properly.

To carry out the performance test, the feedwater system is included by switching on the pump (No, 15), thereby forcing the water into the porous burner (No. 10) until the limit of the level reached. Then, the pump would be stopped automatically. The weight of the tank should be recorded before the boiling test. During the water boiling test, the time that the water level decreases every 1 cm observed through the level sight glass (No. 11) is recorded. To obtain precise and accurate data, each condition must be repeated three times of the testing, and then all data are averaged. In the next step, the gas flow rate is adjusted for the next condition, while the airflow rate is adjusted to obtaining the 7% airflow of the excess O_2 at the flue. The same procedure, as mention above, is repeated three times for each condition.

4. Results and discussion

4.1 Performances of Porous Burner

4.1.1 Combustion and exhaust temperature

The temperature distributions at a steady state of the porous burner (PB) and conventional burner (CB) under the same condition at different the heat loads are presented in Figs. 5 and 6, respectively. They show that the temperature distributions along the combustion chamber of both burner types are proportional to the heat load.

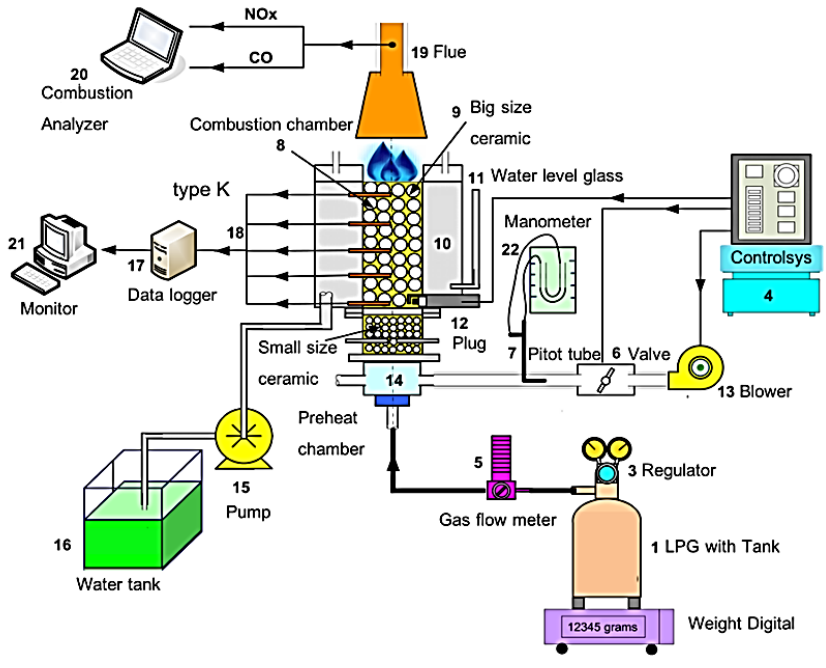

Fig. 4 Schematic diagram of devices and equipment installation

Table 1 Condition for performances of PFTB

Testing Conditions	Porous Burner (PB)	Conventional Burner (CB)
Gas pressure	0.4 bar	0.4 bar
working pressure	1 bar (atm)	1 bar (atm)
Porosity	0.5	1.0
Fuel flow rate	1 – 7 LPM	1 – 7 LPM
Excess O_2 at flue	7%	7%
Water quantity	5 L	5 L
Preheat condition	Yes	No

This can be explained by the fact that gas combustion releases more heat when the amount of fuel-mixture increases. Generally, the temperature distributions of the PB are smoother than those of the CB. At different head loads, the maximum combustion temperature of the PB can be obtained from the highest heat load at a position of x from 5 and 6 cm. This is because of the heat energy stored in this region. Differently, the temperature distributions obtained from the CB type are fluctuating and they drop at x ≈ 5 cm. Besides, the highest temperature is found near the exhaust pipe at the highest heat load. Figs. 5 and 6 also indicate that the maximum temperatures of the PB and CB are in a rank of 815 °C – 1275 °C and 630 °C - 820 °C, respectively. Fig. 7 shows a comparison between the average combustion temperature provided by the PB with that by the CB at different heat loads. One can observe that the average combustion temperatures of both types are proportional to the heat load. In addition, it reveals the PB is more efficient at high heat loads. This phenomenon may be explained by the fact that partial heat generated by porous medium radiates to the fuel-air mixtures in the preheat chamber, thereby enhancing the heat transfer rate inside the porous media. As a result, the combustion temperature of the porous burner increases. To complete the temperature measurement obtained by the combustion process, the exhaust temperatures of the CB and PB under the same condition at different heat loads are compared against each other in Fig. 8. It is found that the exhaust temperature of the PB is lower than that of the CB for all values of the heat load. Interestingly, the flue gas temperatures of the PB and CB are close to each other at high

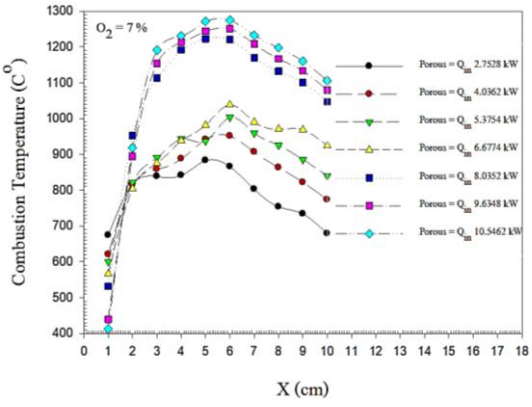

Fig. 5 Temperature distribution of PB

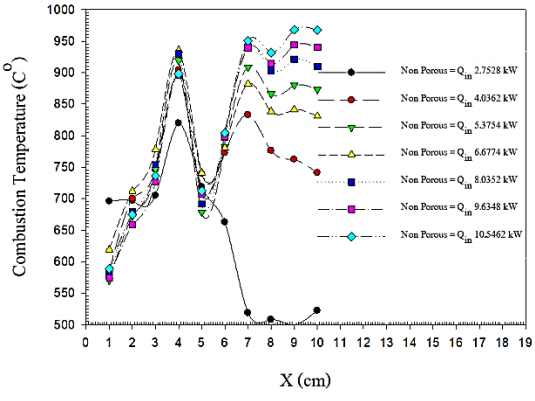

Fig. 6 Temperature distribution of CB

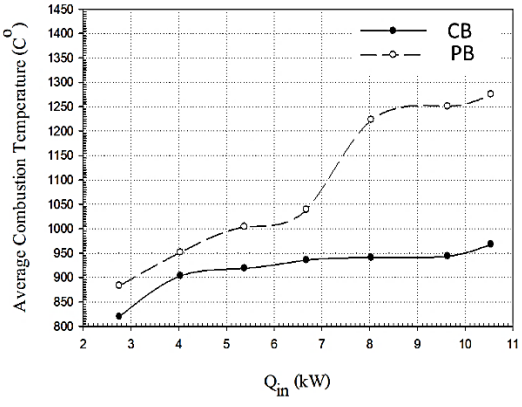

Fig. 7 Average combustion temperature

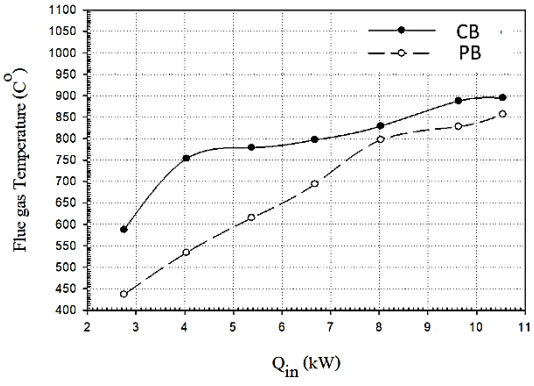

Fig. 8 Flue gas temperature of PB and CB

heat loads, namely, $Q_{in} \geq 8$ kW. Additionally, the exhaust temperature of the PB is about 19% lower than that of the CB on average. The reason for this result is that the flue gas flows slowly through the complicated structure of the porous chamber that has the heat storage and recirculation inside the porous media.

4.1.2 Heat rate, vaporization, thermal efficiency, and energy saving

Fig. 9 illustrates a comparison between the rate of latent heat of the PB and CB at different heat loads. It can be seen that although the latent heat rate of both types increases with the heat load condition with a similar trend, the latent heat rate provided by the PB is 46% higher than that by the CB based on the average value. This result indicates a positive effect provided by the high rate of heat transfer in a porous chamber of the PB thereby causing more efficiency than the free flame in the CB. As a result, the water in a shell of the PB can absorb a higher rate of heat transfer from the porous chamber. Besides, the porous media in the PB contributes to the capability of energy storage, thereby extending the time of heat transfer for more vaporized production, as shown in Fig. 10.

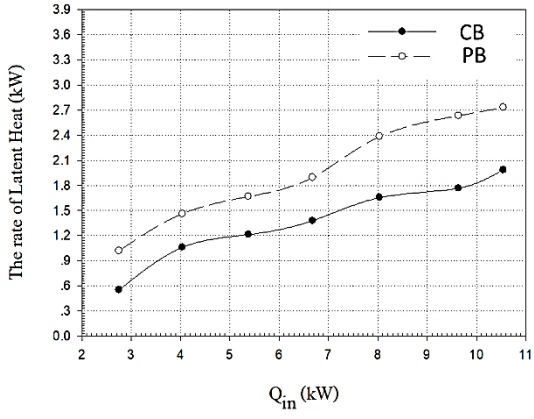

Fig. 9 Heat power output of PB and CB

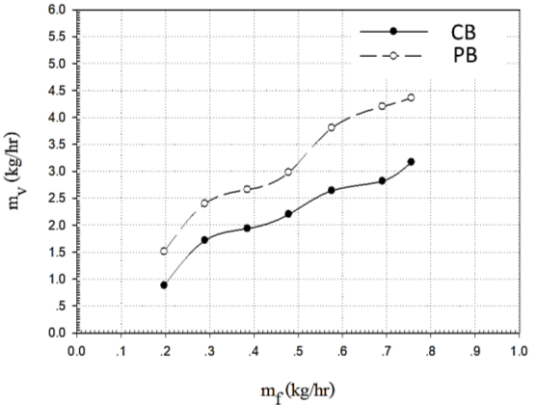

Fig. 10 Steam production of PB and CB

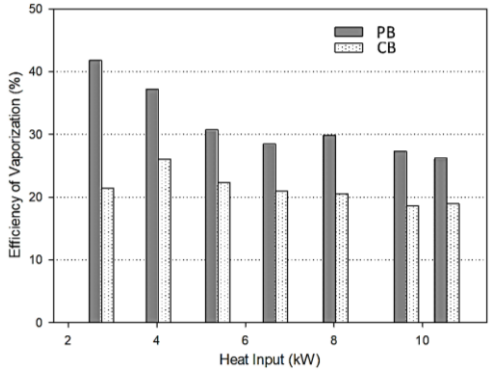

Fig. 11 Thermal efficiency of PB and CB

The results show that on average, the steam produced by the PB is 56% more than that by the CB counterpart. Later, Fig. 11 presents the thermal efficiency of the PB and CB. It is found that the PB type gives a 48.7% averagely higher thermal efficiency than the CB due to a higher efficiency of the PB caused by heat recirculation in the porous layer. Apart from heat rate, vaporization, and thermal efficiency as mentioned above, energy-saving should be considered as well so that it can obtain a better understanding of using the PB when compared to the CB counterpart. Fig. 12 shows energy-saving obtained from the PB and CB and it indicates that energy saving varies with the heat load. On average, the energy saving of the PB is 10.44% better than that of the CB. This suggests that the PB has not only high efficiency but also less fuel consumption than the CB. Also, the use of the PB type at the lowest heat load is very beneficial because it is most economical for energy-saving.

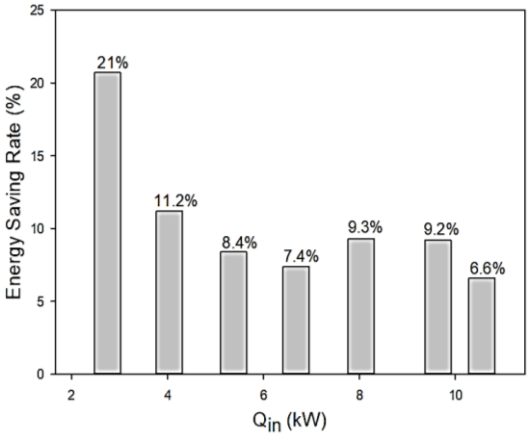

Fig. 12 Higher percentage of energy-saving provided by PB when compared to CB

4.2 CO and NO_x emissions

Figs. 13 and 14 compare the amount of CO and NO_x emitted from using the PB and CB, respectively. These results are conducted at 7% O_2 excess in the flue gas at different heat loads. Surprisingly, Fig. 13 shows that the CO emissions given by the PB at the lowest heat load condition (Q_{in} = 2.75 kW) and the heat load at Q_{in} = 4.00 kW are still high, namely, about 3,600 ppm and 1,750 ppm, respectively. It is quite different from the CO emitted from the CB that is found lower than 300 ppm at Q_{in} = 2.75 kW and very low at higher loads. These results happen because of the low airflow rate at low heat load conditions through the complicated structure of the porous media. This may lead to heterogeneous mixtures between the fuel and air, thereby causing an incomplete combustion. At higher heat loads, the CO emission produced by the PB decreases and very low amounts of CO are noticed.

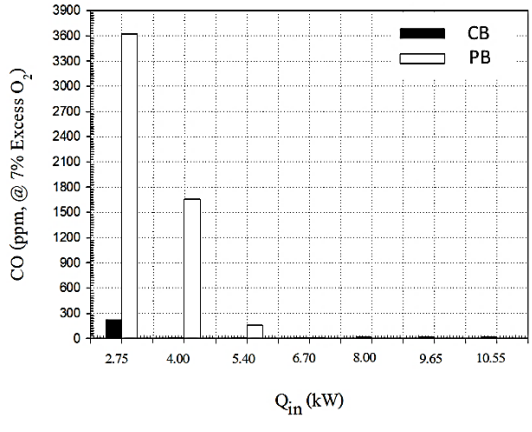

Fig. 13 CO emission of PB and CB

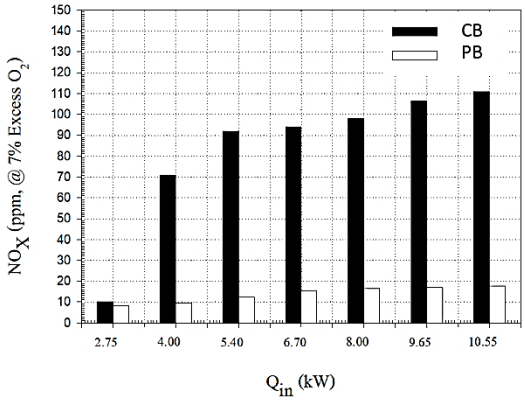

Fig. 14 NO_x emission of PB and CB

Likewise, Fig. 14shows the NO_x emission measured from the PB and CB at 7% O_2 excess in the flue gas at different heat loads. It can be seen that the CB emits the maximum NO_x of about 110 ppm at the highest load (Q_{in} = 10.55 kW), while the maximum of NO_x emission produced by the PB is about 18 ppm at Q_{in} = 10.55 kW. Compared to the NO_x emission by the CB, the amount of NO_x produced by the PB is 75% lower than that by the BC for all conditions. This suggests that with the use of the PB can reduce the NO_x emission significantly. The reason may be due to the increase in NO_x formation at high gas temperatures,

5. Conclusion

This work experimentally studies the performances, energy efficiency, and emissions of a porous burner (PB). The temperature distribution along the porous chamber, the combustion temperature, the latent heat, the water vapor, the capability for vaporization, and the energy-saving, including CO and NO_x emissions are investigated. Also, the results of the PB are compared with those of the conventional burner (CB). Through analysis and discussion, the interesting findings are discovered as follows: 1) the maximum temperatures of the PB and CB are in a range of 815°C - 1275°C and 630°C - 820°C, respectively. 2) On average, the combustion temperature of the PB is about 30% higher than that of the CB at the maximum heat load condition, while the exhaust temperature is about 19% lower than that of the CB based on the average value. 3) The latent energy, vaporization, and thermal efficiency are 46%, 56%, and 48.7% higher than those of the CB, respectively. 4) The energy-saving given by the PB is 10.44% higher than that by the CB. 5) The high CO emissions are observed at low heat loads for the PB but the CO from both PB and CB are not quite different at higher loads. Meanwhile, the amount of NO_x obtained by the PB is dramatically lower than that of the CB, namely, it is lower by 75%. Based on the above results, it suggests that the PB provides not only high efficiency but also less fuel consumption including significant low emission of NO_x.

6. Acknowledgements

This paper is supported by Rajamangala University of Technology Krungthep. Also, the authors would like to thank Dr. Prasert Prapamonthon, Department of Aeronautical Engineering, International Academy of Aviation Industry, King Mongkut's Institute of Technology Ladkrabang for his useful suggestion.

7. References

[1] Howell J, Hall M, Ellzey J. "Combustion of Hydrocarbon Fuels within Porous Inert Media", Progress Energy and

Combustion Science, Volume 22, Issue 2, pp.121-145,1996.

[2] Pantangi V, Mishra S. "Combustion of Gaseous Hydrocarbon Fuels within Porous Media – A Review", Advances in Energy Research, 2006.

[3] Trimis D, Wawrizinek K, Krieger R, Schneider H. "A highly efficient porous radiant burner for industrial applications", Presented at the Sixth European Conference on Industrial Boilers, 2-5 April, 2002.

[4] Liu J, Hsieh W. "Experimental Investigation of Combustion in Porous Heating Burner", Combustion and Flame, Volume 138, pp 295-303, 2004.

[5] Wood S, Harris A. "Porous burners for lean-burn applications", Progress in Energy and Combustion Science 34, pp. 667-684, 2008.

[6] Akbari M, Riahi P, Roohi R. "Lean flammability limits for stable performance with a porous burner", Applied Energy 86, pp. 2635-2643, 2009.

[7] Chu J, Cheng L, Shi Z, Luo Z, Cen Ke-fa. "Experimental Research on a Porous Media Gas-Fired Boiler", Journal of Combustion Science and Technology, 2009-01.

[8] Barcellos W, Souza L, Saveliev A, Kennedy L. "Ultra-low-emission steam boiler constituted of reciprocal flowporous burner", Experimental Thermal and Fluid Science, Volume 35, Issue 3, pp. 570-580, 2011.

[9] Sumrerng J, Viriya N. "Cyclic Operation of Porous Combustor-heater (PCH)", Fuel 88, pp 553 – 559, 2009.

[10] Aekkaphon C, Usa M, Sumrerng J. "Self-aspirating/air-preheating porous medium gas burner", Applied Thermal Engineering 153, pp 181 – 189, 2019